

## Modification of conventional X-ray diffractometer for the measurement of phase distribution in a narrow region

Yang-Soon Park\*, Sun-Ho Han, Jong-Goo Kim, Kwang-Yong Jee and Won-Ho Kim

*Korea Atomic Energy Research Institute, 150 Deokjin-dong, Yuseong-gu, Daejeon, 305-353, Korea*

(Received August 29, 2006; Accepted September 22, 2006)

**Abstract:** An X-ray diffractometer for spatially resolved X-ray diffraction measurements was developed to identify phase in the narrow (micron-scaled) region of high burn-up fuels and some nuclear materials. The micro-XRD was composed of an X-ray microbeam alignment system and a sample micro translation system instead of a normal slit and a fixed sample stage in a commercial XRD. The X-ray microbeam alignment system was fabricated with a microbeam concentrator having two Ni deposited mirrors, a vertical positioner, and a tilt table for the generation of a concentrated microbeam. The sample micro translation system was made with a sample holder and a horizontal translator, allowing movement of a specimen at 5  $\mu\text{m}$  steps. The angular intensity profile of the microbeam generated through a concentrator was symmetric and not distorted. The size of the microbeam was  $4,000 \times 20 \mu\text{m}$  and the spatial resolution of the beam was 47  $\mu\text{m}$  at the sample position. When the diffraction peaks were measured for a  $\text{UO}_2$  pellet specimen by this system, the reproducibility ( $2\theta = \pm 0.01^\circ$ ) of the peaks was as good as a conventional X-ray diffractometer. For the cross section of oxidized titanium metal, not only  $\text{TiO}_2$  in an outer layer but also  $\text{TiO}$  near an oxide-metal interface was observed.

**Key words:** micro X-ray diffraction, microbeam concentrator, narrow region, interface

### 1. Introduction

Great efforts have been made to reduce fuel cycle costs, and it has been found that it could be achieved by increasing the burn-up of the fuel. Increasing the burn-up of the fuel produces a large amount of fission products thus causing damage to the fuel rods. Thus numerous studies have been carried out to analyze the safety of spent fuels at a high burn-up. It has been observed that microstructure changes occur at the radial edge of a pellet (rim) of the fuel at a high burn-up.<sup>1</sup> The thickness of a rim is some

hundreds of micrometers. Despite its narrow region, a rim would affect the behavior of a nuclear fuel. Thus, identifying the crystal structure change in a rim is needed at intervals as small as 30-50  $\mu\text{m}$ , and a microbeam is needed.<sup>2</sup> The line type and concentrated microbeam is effective to detect the XRD peak intensities of a high burn-up fuel because its peak intensities are reduced to about a tenth by the irradiation damage causing the increased porosity, the decreased hardness, the lattice distortion, etc., that is not available commercially.

Optics such as mirrors and lens to generate an X-

★ Corresponding author

Phone : +82-(0)42-868-8285 Fax : +82+(0)42-868-8148

E-mail: nyspark@kaeri.re.kr

ray microbeam are divided into three groups of the grazing incidence mirrors,<sup>2-9</sup> the diffractive mirrors,<sup>10-12</sup> and the refractive lens.<sup>13</sup> The grazing incidence mirrors which rely on the principle that the X-rays can be reflected from a smooth surface at less than the critical angle are classified into an oblong metal mirror, capillary concentrator, ellipsoidal mirror, Wolter mirror, and microchannel array. The diffractive mirrors which rely on the Bragg reflection are classified into crystal mirror, multilayer mirror, Fresnel zone plate, and Bragg Fresnel lens. The refractive lens which relies on the difference in the refractive index between air and the lens material is a compound refractive lens consisting of tens or hundreds of individual lenses arranged in a linear array. The diffractive mirrors and the refractive lens need high input X-ray intensities due to the loss of the beams and they are usually connected to a synchrotron radiation source. Therefore, the grazing incidence mirrors relying on a total reflection are effective for obtaining the microbeam concentrated with a conventional X-ray source.<sup>14</sup> Generally, a high electron density metal (Pt, Au, Ni, etc.) has a high critical angle ( $\theta_c$ ) for a total reflection.<sup>2</sup> D. Papaioannou developed a collimating system with Ni metal plates as the grazing incidence mirrors to condense hard X-ray. The collimating system provides a very thin, intense, and low divergent beam by two oblong and flexible Ni metallic mirrors with an exit aperture  $4 \text{ mm} \times 15 \mu\text{m}$ .<sup>2</sup> D. Papaioannou attached this concentrator to a shielded X-ray diffraction system, and analyzed two fuel samples with 67 and 80 GWd/tM average burn-ups at  $50 \mu\text{m}$  intervals.

In this article, Ni deposited glass plates were used as mirrors to concentrate hard X-ray from a conventional X-ray diffraction system. The mirrors were manufactured by a Ni deposition (below  $1 \mu\text{m}$  in thickness) on two oblong, polished and flexible glass plates. The micro-XRD system was composed of an X-ray microbeam alignment system and a sample micro translation system, and its apparatus is described and its performance results are discussed.

## 2. Development of a micro X-ray diffractometer

### 2.1. X-ray microbeam alignment system

The X-ray microbeam alignment system was composed of a microbeam concentrator and a concentrator alignment part. The microbeam concentrator was fabricated with two Ni deposited mirrors, an exit slit, and a housing to protect the mirrors. Ni deposited glass plates were used as mirrors to make a more flexible mirror and a more easily polished surface than the Ni metal plate. The concept of a microbeam concentration is the total reflection principles on two opposite Ni deposited mirrors (*Fig. 1*). Since the critical angle ( $\theta_c$ ) for Ni at the Cu characteristic line (8 keV) is about  $0.42^\circ$ , the incident X-ray beam below  $0.42^\circ$  on the Ni surface can be reflected and concentrated. The mirrors were prepared by a deposition (about  $0.7 \mu\text{m}$  in thickness) of Ni to the surface of two oblong, flexible and polished glass plates. They were deposited below  $1 \mu\text{m}$  in thickness to reduce the surface stress of the flexed mirrors. The mirrors were manufactured to  $130 \times 8 \times 1 \text{ mm}$  dimensions after a consideration of the distance between an X-ray tube and a sample position. An entrance opening of the concentrator of about  $0.3 \text{ mm}$  was permitted for a concentrator length of about  $130 \text{ mm}$  because the critical angle ( $\theta_c$ ) of the X-ray for Ni is  $0.42^\circ$ .<sup>2</sup> The exit opening of two mirrors was generated with two Pt foils ( $50 \mu\text{m}$  in thickness) between two mirrors (*Fig. 2*). An antidivergence slit of  $20 \mu\text{m}$  in width was placed at the concentrator exit to maintain the central core of the concentrated beam. To ensure a safe handling of the concentrator, the two mirrors are set in an

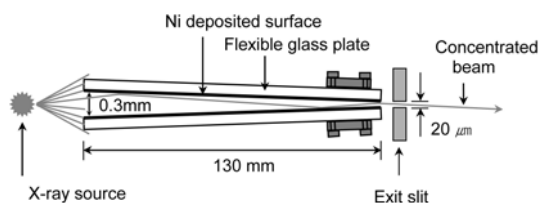


*Fig. 1.* Concentration of the X-ray beam between two oblong flexible mirrors.

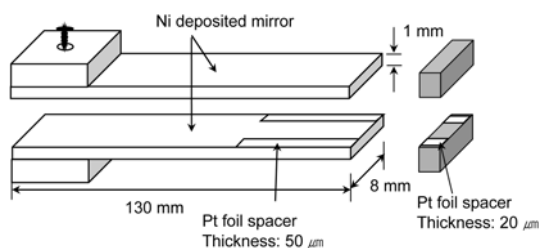


Fig. 2. Generation of the micro beam ( $20\ \mu\text{m}$  width) with the thin foil spacers (Pt).

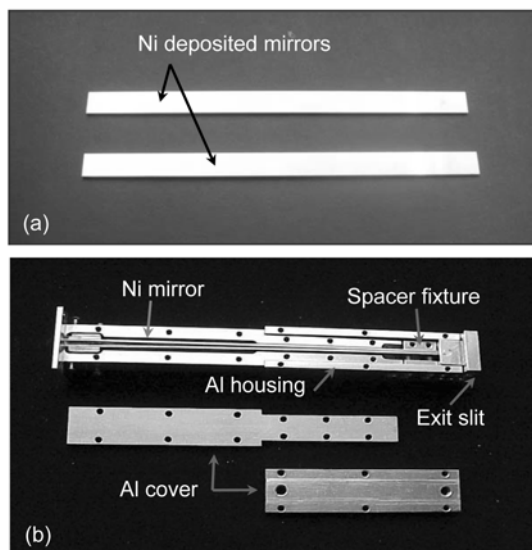


Fig. 3. Ni deposited mirrors (a) and an X-ray microbeam concentrator which consisted of two mirrors, a spacer fixture, an exit slit and an aluminum housing (b).

aluminum housing (Fig. 3). The mirrors were aligned with a vertical positioner (travel length: 6 mm, sensitivity:  $0.5\ \mu\text{m}$ , repeatability:  $2.5\ \mu\text{m}$ , ORIEL) to control the height and the tilt table (tilt adjustment:  $\pm 2.5^\circ$ , sensitivity:  $1.25\ \mu\text{rad}$ , ORIEL) to control the slope (Fig. 4). The microbeam alignment system was attached to an X-ray tube with the connectors of an 'L' type.

## 2.2. Sample micro translation system

The sample micro translation system was composed of a sample holder (dimension:  $40 \times 46 \times 53\ \text{mm}$ ) and a horizontal translator (travel length: 12.7 mm, sensitivity:  $0.8\ \mu\text{m}$ , repeatability:  $2.5\ \mu\text{m}$ , ORIEL) as shown in Fig. 5. The sample holder could set a specimen of 12-32 mm diameter and 1-

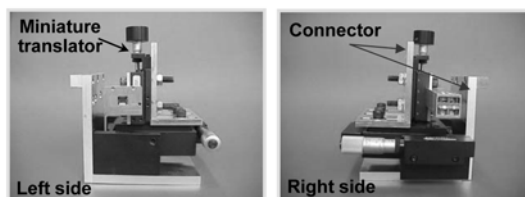
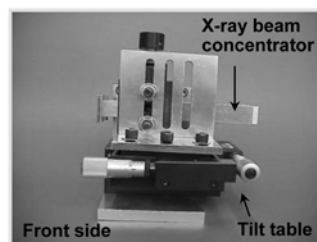


Fig. 4. Microbeam alignment system which consisted of a microbeam concentrator, a vertical positioner and a tilt table.

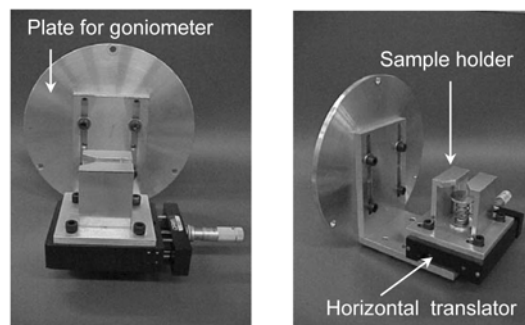


Fig. 5. Sample micro translation system with a sample holder and a horizontal translator.

30 mm height. It was made of aluminum, open at a wall and easy for setting a sample in, fixed with bolts to a horizontal translator and it could be moved at 5  $\mu\text{m}$  steps. The sample micro translation system was attached to a goniometer with the connectors of an 'L' type and a round shape.

Finally, the micro-XRD system was composed of the X-ray microbeam alignment system and the sample micro translation system instead of the normal slit and the fixed sample stage of a conventional XRD (D5000, SIEMENS) as shown in Fig. 6.

## 2.3. Characterization of the generated microbeam

### 2.3.1. Beam intensity

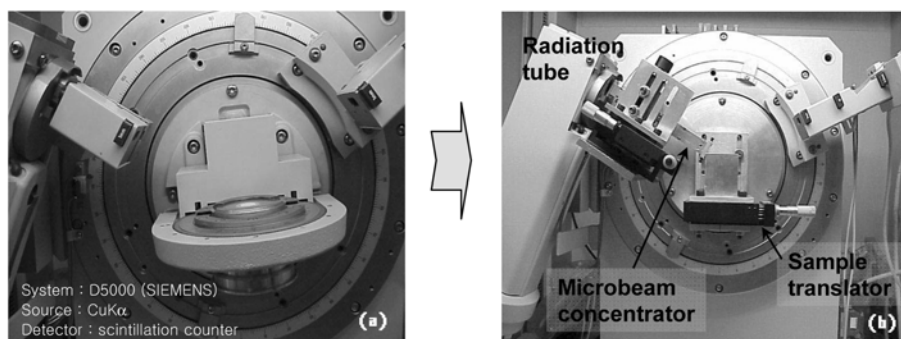


Fig. 6. Conventional X-ray diffractometer (a) and a micro X-ray diffractometer with a microbeam concentrator alignment system and a sample micro translation system (b).

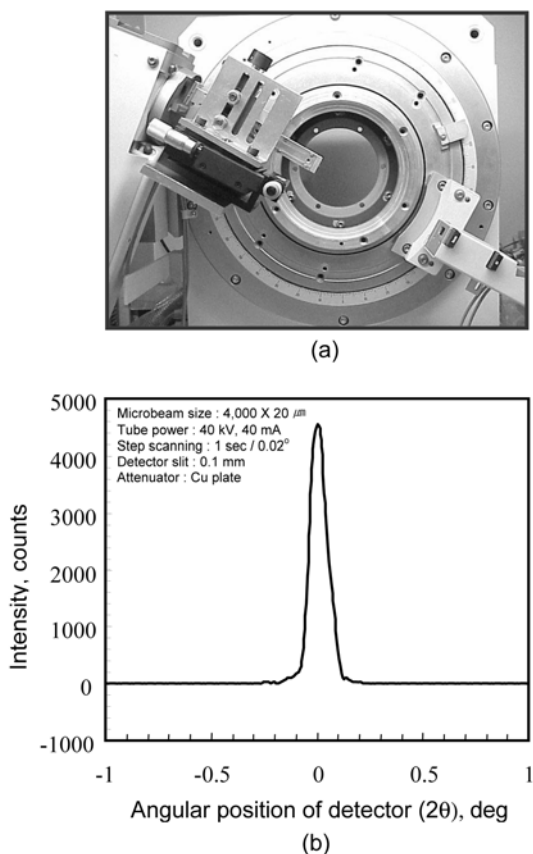


Fig. 7. Beam direct detection system (a) and an intensity profile of the microbeam observed by an angular detector scanning (b).

The intensity profile of the generated microbeam was observed at a distance of about 230 mm from exit slit by an angular detector scanning ( $2\theta = -1^\circ \sim$

$+1^\circ$ ). A receiving slit of 0.1 mm in width was used for the measurement and a copper foil was placed as an attenuator in front of a detector to avoid any detector damage. Other operating conditions were the same as a routine x-ray diffraction analysis condition. As shown in Fig. 7, the developed microbeam alignment system provided a symmetric microbeam without a distortion and background level increase. The intensity gain of the microbeam concentrator was determined by total intensity detected with a receiving slit of 6 mm in width. The other measuring conditions were the same as above. The intensity gain of the microbeam concentrator was about five times (about 25,000 counts/s) that of the value (about 5,000 counts/s) measured without mirrors through a simple slit of the same aperture dimensions.

### 2.3.2. Spatial resolution of the X-ray microbeam

The spatial resolution is the width of the X-ray microbeam irradiated to the surface of a sample. After the generation of a microbeam with 20  $\mu\text{m}$  in width, the spatial resolution was determined experimentally at an incident angle ( $\theta$ ) with a reference sample under the same operating conditions of a routine X-ray diffraction analysis.<sup>2</sup> An  $\text{Al}_2\text{O}_3$  and a  $\text{MgAl}_2\text{O}_4$  single crystals (5 mm  $\times$  5 mm  $\times$  1 mm) molded with epoxy resin were used as the reference samples. The specimen was placed on a sample micro translation stage and the measurements were performed. The diffraction peaks of the  $\text{Al}_2\text{O}_3$  single crystal were measured at 5  $\mu\text{m}$  steps (at an incidence

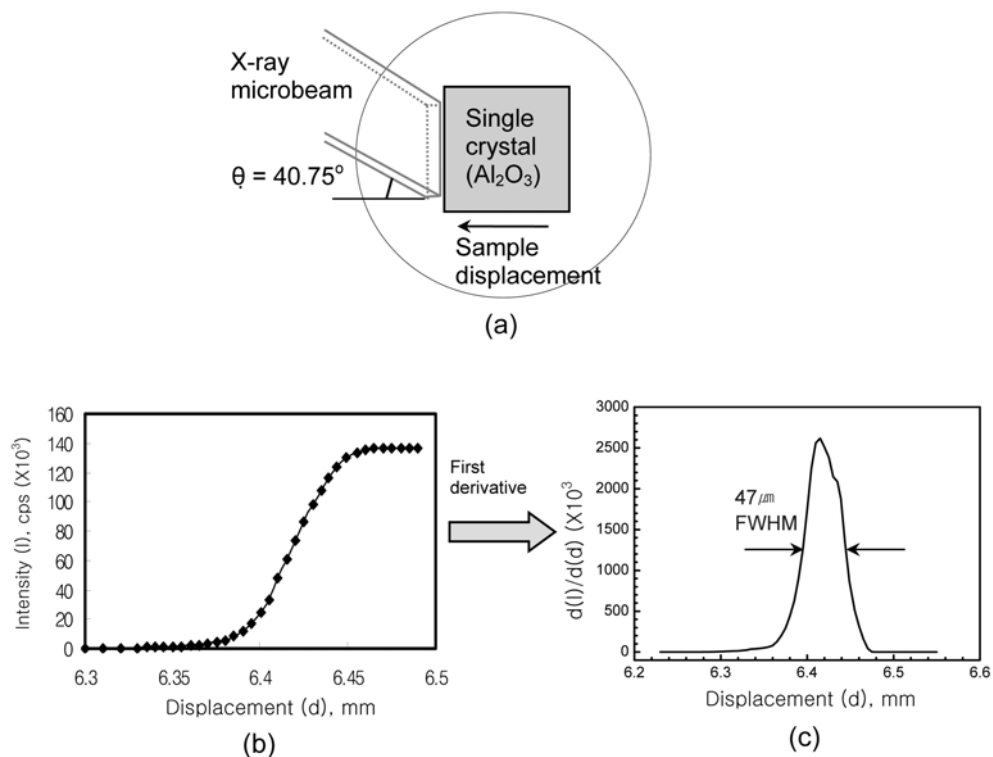


Fig. 8. Spatial resolution determination of the X-ray microbeam. (a): Al<sub>2</sub>O<sub>3</sub> single crystal reference sample, (b): Diffraction peak intensity at an incident angle  $\theta = 40.75^\circ$  as a beam spot location on the sample, (c): Beam spot thickness (FWHM) at an incident angle  $\theta = 40.75^\circ$

angle ( $\theta$ ) of  $40.75^\circ$ ). The diffraction peak intensity was increased from the background level to a maximum value, when the incident beam was irradiated fully on the Al<sub>2</sub>O<sub>3</sub> single crystal (Fig. 8). The spatial resolution of the generated microbeam

(20  $\mu\text{m}$  width) was 47  $\mu\text{m}$  at  $\theta = 40.75^\circ$ , FWHM(Full Width Half Maximum) of the peak by a differentiation of the curve. It is about twice that of the value obtained through two Ni metallic mirrors.<sup>2</sup> The other spatial resolutions were determined at  $\theta = 9.5^\circ$  (MgAl<sub>2</sub>O<sub>4</sub>),  $18.89^\circ$  (Al<sub>2</sub>O<sub>3</sub>) and  $35.75^\circ$  (Al<sub>2</sub>O<sub>3</sub>). The plot of the spatial resolutions was obtained as a function of the incident angle (Fig. 9). In Fig. 9, the spatial resolution showed an exponential decrease as the incident angle increased, which was about 400  $\mu\text{m}$  at  $\theta = 10^\circ$  but it abruptly decreased to 50  $\mu\text{m}$  at  $\theta=20^\circ$ . The spatial resolution of the microbeam was 47-50  $\mu\text{m}$  for  $\theta>20^\circ$ .

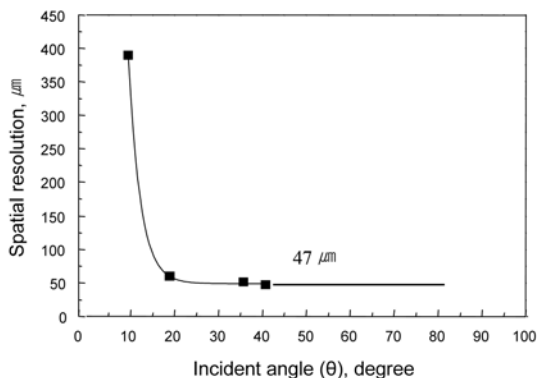


Fig. 9. Spatial resolution of a micro beam as an incident angle ( $\theta$ ) on the surface of a single crystal reference sample.

### 3. Evaluation of a developed micro X-ray diffractometer

#### 3.1. Lattice parameter determination in the micro region of a UO<sub>2</sub> pellet

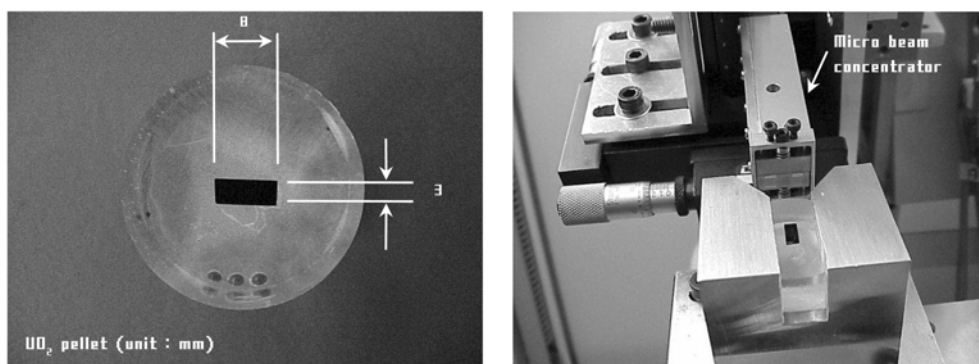


Fig. 10.  $\text{UO}_2$  pellet specimen on a sample micro translation system.

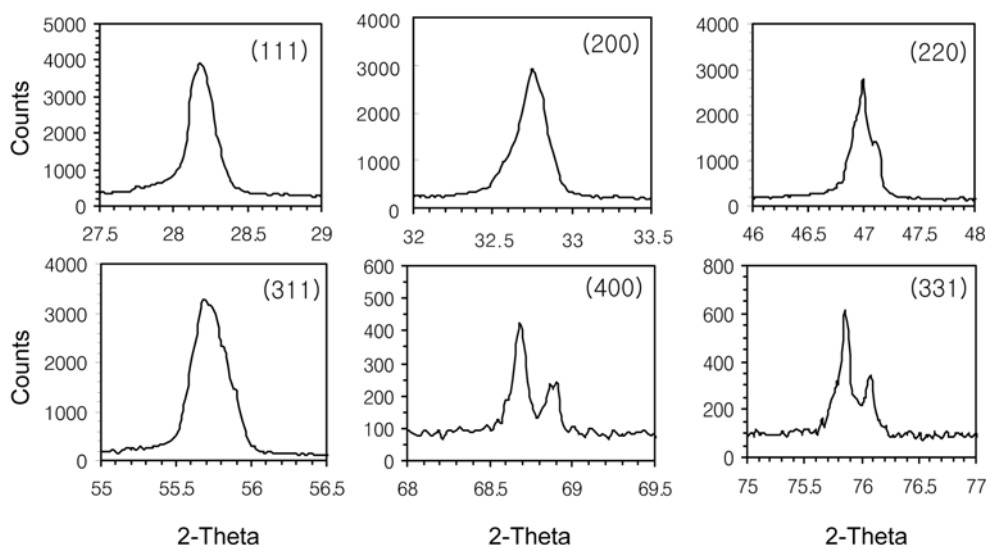


Fig. 11. Diffraction peaks of the  $\text{UO}_2$  pellet specimen by micro-XRD.

The diffraction pattern of  $\text{UO}_2$  was measured by the micro-XRD and its lattice parameter was obtained with 'POWDER' program (crystal system: cubic, space group:  $Fm\bar{3}m$ , lattice parameter (a): 5.467). The  $\text{UO}_2$  pellet specimen was prepared by cutting a pellet to  $8 \times 3$  mm in size, molding it with epoxy resin, and polishing (Fig. 10). The X-ray source used for the measurement was the  $\text{CuK}\alpha$  line, the x-ray generation power was 40 kV, 40 mA, the microbeam size was  $4 \text{ mm} \times 20 \mu\text{m}$ , the measuring time/step was  $40 \text{ sec./}0.02^\circ(2\theta)$ , the filter used to eliminate a  $\text{CuK}\beta$  line was Ni foil, the detection slit width was 0.6 mm and the scanning range was  $20^\circ < 2\theta < 80^\circ$ . As shown in Fig. 11, the diffraction peaks

for the face-centered-cubic (fcc) phase of  $\text{UO}_2$  were detected and the intensity of the peaks was in the 350-3800 count range. Because the diffraction peak can be detected when the peak intensity is two or three times that of the noise, the detection limit is about 40 counts for the optimum measuring condition. Therefore, it is possible that most of the diffraction peaks for a high burn up  $\text{UO}_2$  fuel could be measured by the developed micro-XRD though its peak intensities are reduced to about a tenth due to irradiation damage.<sup>1</sup> When the diffraction peaks were measured for three times at the same position of the  $\text{UO}_2$  specimen, the precision of the peaks was  $\pm 0.01^\circ$  and that of the lattice parameters was  $\pm$

0.0001 Å. This means that the developed micro XRD have the same reproducibility as a conventional XRD with a normal wide beam. When the diffraction peaks were measured for seven points of the UO<sub>2</sub> specimen at 500 μm intervals, the lattice parameters were in 5.4681±0.0009 Å range. These values obtained with the microbeam appeared to be less precise due to the small size of the irradiated area than the normal beam (1 mm slit width, 5.4694 ± 0.0001 Å).

### 3.2. Material characterization near the metal-oxide interface of an oxidized Ti specimen

The optical micrograph for the cross section of the oxidized titanium specimen is shown in Fig. 12(a). The specimen was prepared from Ti metal plate (10 × 9 mm) of a 3 mm thickness by a heat treatment in a muffle furnace under an atmospheric condition. Ti (99.5%, Nilaco) plate was heated for 30 minutes at 1100°C. The oxidized sample specimen was sectioned

horizontally, molded by epoxy resin, and then polished. The measurement was carried out with a scanning step of 0.04° for 40s per each count in the scanning range of 25° < 2θ < 45°.

The XRD patterns measured at various positions (Fig. 12(a)) by the micro-XRD system are shown in Fig. 12(b). In the outer layer of the oxidized specimen, only TiO<sub>2</sub> was observed. Near metal-oxide interface, TiO started to appear and it was increased in deeper layer. TiO was not observed at position about 300 μm from the oxide-metal interface and only Ti metal was observed. It means that TiO<sub>2</sub> was produced in the outer layer of titanium metal by thermal oxidation and TiO also was produced in the layer inside an oxide-metal interface by oxygen diffusion into Ti metal in an environment of oxygen-deficiency.

## 4. Conclusion

The micro-XRD system developed in this study generates an X-ray microbeam concentrated with two Ni deposited mirrors and it can move a sample at steps as small as 5 μm. The generated microbeam has 4,000 × 20 mm dimensions through an exit slit and a 47 μm spatial resolution at the sample position. For a UO<sub>2</sub> pellet specimen, the reproducibility (2θ = ± 0.01°) of the peaks was as good as a conventional X-ray diffractometer. For the cross section of an oxidized titanium metal by this system, not only TiO<sub>2</sub> in an outer layer but also TiO near an oxide-metal interface was determined.

Therefore, this micro-XRD system is applicable to the analysis of oxide layers of tubes (or metal plates) and layers of sandwich materials at 50 μm intervals. In the future, the developed micro-XRD system will be installed with a gamma shielding, and a crystal structure change in the narrow region of high burn-up fuels, clad and the radioactive samples will be identified with this shielded system at 50 μm intervals.

## Acknowledgments

This work was performed under the Nuclear R&D

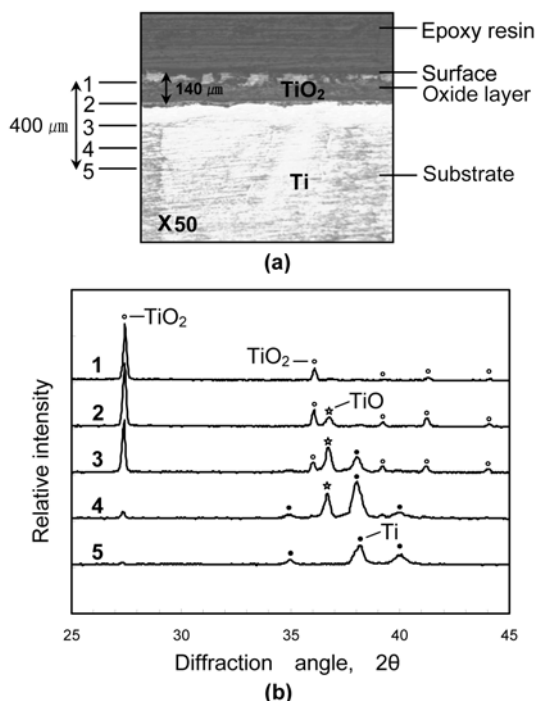


Fig. 12. X-ray diffraction patterns at various positions (100 μm intervals) of the cross section of the oxidized Ti metal by micro-XRD.

Programs sponsored by the Ministry of Science and Technology of Korea

## REFERENCES

1. J. Spino and D. Papaioannou, *Journal of Nuclear Materials*, **281**, 146-162 (2000).
2. D. Papaioannou and J. Spino, *Review of Scientific Instruments*, **73**, 2659-2665 (2002).
3. D. H. Bilderback and D. J. Thiel, *Review of Scientific Instruments*, **66**, 2059-2063 (1995).
4. Y. Suzuki and F. Uchida, *Review of Scientific Instruments*, **63**, 578-581 (1992).
5. M. R. Howells, D. Cambie, R.M. Duarte, S. Irick, A.A. MacDowell, *Opt. Eng.* **39**, 2748-2762 (2000).
6. A. Takeuchi, Y. Suzuki, K. Uesugi, and S. Aoki, *Nuclear Instruments and Methods in Physics Research A*, **467-468**, 302-304 (2001).
7. S. Hayakawa, A. Iida, S. Aoki, and Y. Gohshi, *Review of Scientific Instruments*, **60**, 2452-2455 (1989).
8. H. N. Chapman, K. A. Nugent, and S. W. Wilkins, *Applied Optics*, **32**, 6316-6332 (1993).
9. H. N. Chapman, A. Rode, K. A. Nugent, and S. W. Wilkins, *Applied Optics*, **32**, 6333-6340 (1993).
10. P. Dhez, P. Chevallier, T. B. Lucatorto, and C. Tarrío, *Review of Scientific Instruments*, **70**, 1907-1920 (1999).
11. A. Snigirev, *Review of Scientific Instruments*, **66**, 2053-2058 (1995).
12. C. David and A. Souvorov, *Review of Scientific Instruments*, **70**, 4168-4173 (1999).
13. A. Snigirev, V. Kohn, I. Snigireva, and B. Lengeler, *Nature*, **364**, 49-51 (1996).
14. Y. S. Park, Y. K. Ha, S. D. Park, S. H. Han, and W. H. Kim, "X-ray microbeam generation with optical mirrors and lens", KAERI/AR-706/2004, Korea Atomic Energy Research Institute, 2004.